Quantum quenches in two spatial dimensions using chain array matrix product states

A. J. A. James and R. M. Konik

Phys. Rev. B **92**, 161111 — Published 15 October 2015

DOI: 10.1103/PhysRevB.92.161111

Quantum quenches in two spatial dimensions using chain array matrix product states

A. J. A. James
*London Centre for Nanotechnology, University College London, Gordon Street, London WC1H 0AH, United Kingdom**

R. M. Konik
CMPMS Department, Brookhaven National Laboratory, Upton, New York 11973, USA
(Dated: September 10, 2015)

We describe a method for simulating the real time evolution of extended quantum systems in two dimensions. The method combines the benefits of integrability and matrix product states in one dimension to avoid several issues that hinder other applications of tensor based methods in 2D. In particular it can be extended to infinitely long cylinders. As an example application we present results for quantum quenches in the 2D quantum (2+1 dimensional) Ising model. In quenches that cross a phase boundary we find that the return probability shows non-analyticities in time.

PACS numbers: 05.70.Ln,02.70-c,05.30.Fk

The advent of ultra cold atomic gas experiments has led to a surge of interest in the time evolution and out-of-equilibrium behaviour of many-body quantum systems. Much effort has been focused on one dimensional (1D) problems because these can be tackled by analytically tractable or highly accurate numerical methods. Key questions that these studies have sought to elucidate are whether and how such systems thermalise after a sudden change, or 'quantum quench' of a system's Hamiltonian; with particular emphasis on the role played by conserved charges in 1D integrable systems [1–11].

Experiments however, are not limited to 1D and it is interesting to explore similar questions in two dimensions (2D) and above [12]. Unfortunately there is no analogue in 2D of the aforementioned analytically exact 1D methods. Numerical approaches using matrix product state (MPS) representations, so successful in 1D, suffer in 2D due to the 'area law' growth of entanglement [13, 14]. This growth reduces the efficiency of MPS (and related 'tensor') algorithms and limits them to smaller system sizes.

Nonetheless MPS algorithms can be applied in 2D, by labeling lattice sites (usually in a zigzag fashion) to map to a 1D system [15]. The cost is that nearest neighbor interactions in 2D are mapped to increasingly long ranged 1D interactions, imposing an increasing numerical burden. Recently progress has been made in performing real time evolution on MPS with such long ranged Hamiltonians by two different routes [16, 17]. Algorithms based on generalizations of MPS to higher dimensions, such as projected entangled pair states (PEPS) [18, 19], make use of imaginary time evolution to find ground states [20]. However these higher dimensional tensor methods have not been applied to real time evolution.

In this letter we demonstrate that *real* time evolution is possible for large 2D systems by combining information coming from exactly solvable models with a highly anisotropic MPS formulation. Such an approach retains the contraction efficiency of matrix product states over other tensor methods, while avoiding the build up of long ranged interactions. Our setup will be similar to that used in the density matrix renormalisation group (DMRG) studies described in Refs. [21, 22] except that here we are explicit in our use of MPS. This change allows for straightforward implementation of algorithms other than DMRG, including those for time evolution and for accurately working with the thermodynamic limit. In particular using time evolving block decimation (TEBD) [23] we demonstrate that we can study the time evolution after a quench of infinitely long cylinders, with sufficient circumference that we approach the 2D thermodynamic limit. This includes strong quenches where we cross phase boundaries of a 2D quantum system.

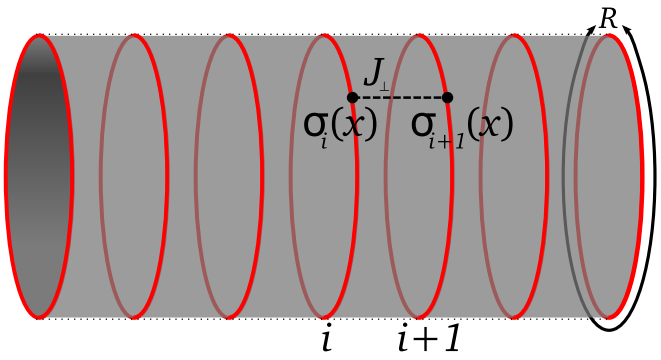

FIG. 1. Anisotropic setup for a 2D system as an array of N chains of length R, coupled by an interaction $J_\perp$. The cylinder can be joined together at its ends to study toroidal systems.

Method: At the core of our method is the wish to maximise the analytically exact input going into our MPS algorithm, while simultaneously controlling the growth of entanglement entropy. The construction we use is depicted in Fig. 1: a coupled array of *exactly solvable* 1D subunits. For each subunit, we have *exact* knowledge of

the spectrum and matrix elements. This exact knowledge means that we begin with the numerics already having accounted for much of the strong correlations of the system. We emphasize our use of exactly solvable models as a building block is not much of a limitation to the method. Such models are ubiquitous in 1D, including Heisenberg spin chains, Luttinger liquids, and Hubbard models to name but a few [24, 25]. In this framework, a state of a system of N chains is written in MPS form via

$$|\Psi\rangle_{\rm 2D} = \sum_{\boldsymbol{\sigma}} A^{\sigma_1[1]} \cdots A^{\sigma_N[N]} |\sigma_1 \cdots \sigma_N\rangle \qquad (1)$$

where each matrix $A^{\sigma_i[i]}$ is labelled by a chain i and an eigenstate of that individual chain σ_i. Like the single sites used in 1D MPS algorithms, we are able to manipulate these chain eigenstates because we know their energies and matrix elements for any relevant operator.

For ground and low-lying states of the system the entanglement entropy S_E scales as the boundary 'area', that is to say the chain length. By keeping the chain length finite we can throttle the growth of S_E. By partnering this with the fact that for the systems that we will study, finite size effects are *exponentially suppressed*, we are able to keep S_E small while remaining in the 2D thermodynamic limit. We have previously demonstrated the effectiveness of this methodology in equilibrium by studying a 2D quantum (i.e. $2+1$ dimensional) critical point [21, 22].

The continuum 1D subunits will necessarily have an infinitely large Hilbert space. However if the system size R is finite the spectrum is discrete, and we may truncate at a cutoff energy E_c. This step is justified by appeal to the truncated conformal spectrum approach [26] where it has been observed over a wide body of examples [27–29] that for *relevant* (in the renormalisation group sense) interchain interactions, the low energy sector of a perturbed integrable system is formed primarily from (possibly strong) admixtures of low lying states of the unperturbed system. Here we will focus on exactly such interchain perturbations.

Eq. 1 differs from a MPS for a 1D system only in that the 'physical indices' σ may be large (see Table 1 of [30]), requiring strict use of sparse matrices to maximise computational resources. It is also important to take advantage of good quantum numbers and to perform matrix operations (e.g. singular value decompositions) in a block diagonal manner, to help preserve the sparse nature of the matrices and increase numerical efficiency.

MPS time evolution algorithms may then be implemented just as for a 1D system, including TEBD [23] and its infinite counterpart (iTEBD) [31, 32]. For the former we may work with a torus or open cylinder geometry; the latter corresponds to an infinitely long cylinder. Both algorithms decompose the time evolution operator $\exp[-iHt]$ into a product of N_t time step operators, $t = N_t\tau$. Each step is itself approximately decomposed into a product of two site (or chain) operations. The error at each step is proportional to the time increment τ raised to a power given by the order of the decomposition.

A more important source of error is the compression of the MPS after each step via Schmidt decompositions. We compress by fixing a minimum singular value size, s_{min}: singular values smaller than this threshold value are discarded. In this sense our algorithm is adaptive, as χ, and the degree of encoded entanglement can grow. 'Lieb-Robinson' type arguments limit the rate of growth of S_E after a quench [33–35], but χ may grow exponentially, limiting the maximum timescales that can be reached.

For our 2D algorithm, forming the time evolution operator requires the exponentiation of a two chain Hamiltonian, which in turn necessitates the diagonalisation of the same object. This is a numerically costly step, but need only be done once at the beginning, and the result stored for later use.

In this letter we present results for quenches in the 2D quantum Ising model:

$$H_{\rm 2DQI} = \sum_i \left[H_{{\rm 1D},i} + J_\perp \int_0^R {\rm d}x \; \sigma_i^z(x)\sigma_{i+1}^z(x) \right]. \qquad (2)$$

We represent the model as 1D Ising chains (of index i and length R) coupled together with a longitudinal spin-spin interaction. We take each chain $H_{{\rm 1D},i}$ to be the continuum limit of the 1D lattice quantum Ising model—or transverse field Ising model (TFIM)—with Hamiltonian, $-J_\parallel \sum_l [\sigma_{i,l}^z \sigma_{i,l+1}^z + (1+g)\sigma_{i,l}^x)]$ with l an index along the chain. In the continuum limit this reduces to a theory of a 1D Majorana field with mass $\Delta = gJ_\parallel$. Analytic expressions for the spectrum of this theory and the spin matrix elements are detailed in Ref. [36]; we summarize the salient features in [30]. Expanding the Majorana field in terms of fermionic modes $\psi_{k_i}^\dagger$ and ψ_{k_i} (the continuum versions of the usual Jordan-Wigner lattice fermions) yields a quadratic chain Hamiltonian $H_{{\rm 1D},i} = \sum_{k_i} \epsilon_{k_i} \psi_{k_i}^\dagger \psi_{k_i}$, with dispersion $\epsilon_{k_i} = \sqrt{\Delta^2 + k_i^2}$. We work in units such that the *intrachain* velocity, v, is dimensionless and equal to unity. We also define a dimensionless interchain coupling $j_\perp = J_\perp |\Delta|^{-7/4}$. For disordered ($\Delta < 0$) chains a finite value of the interchain coupling $j_\perp$ leads to a 2D quantum (d=2+1) order-disorder transition at a critical value $j_\perp = j_c = 0.185$ [22].

We compute the evolution of the postquench state using iTEBD and TEBD, with first and second order Trotter decompositions of the time evolution operator, and time steps τ. The error associated with such decompositions is dependent on $j_\perp$ and τ, but even for the strongest quenches presented in this work we can choose τ small enough for convergence (see the supplementary material [30]). For each set of parameters, we first establish that the numerical results are converged in s_{min} or χ before increasing the cutoff E_c. Convergence of the method in s_{min} is demonstrated in [30]. We have also checked the

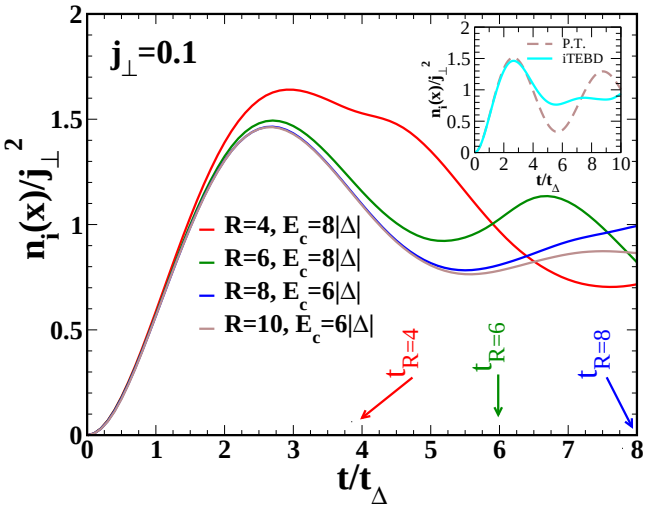

FIG. 2. Fermion occupation number, $n_i(x)$ scaled by interchain coupling, $j_\perp^2$. We indicate the time scale t_R at which we expect the system postquench to see the effects of the finite circumference of the system. Inset: $R = 10$ iTEBD data compared with the perturbative result (P.T.) (dashed line).

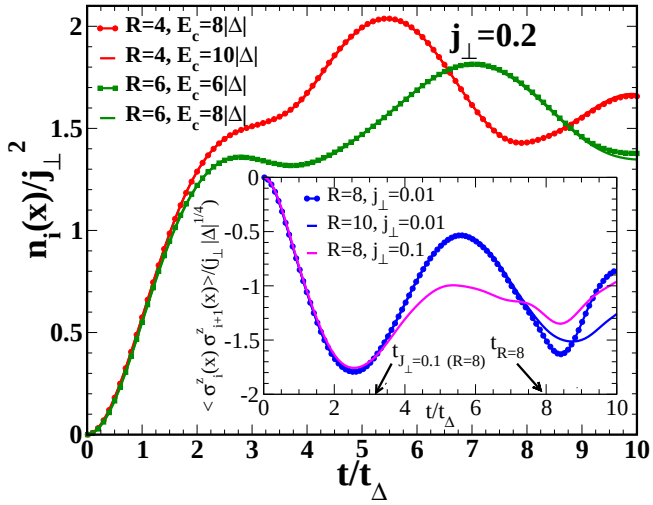

FIG. 3. Fermion occupation number, $n_i(x)$, scaled by interchain coupling, $j_\perp = 0.2$, squared. Curves for different E_c are shown, corresponding to more than doubling the number of retained states in the chain spectrum. The agreement is excellent until the latest times, even though this quench crosses a critical point. Inset: the nearest neighbor spin-spin correlation function showing scaling with $j_\perp$ and R.

algorithm for two analytically tractable cases: the perturbative limit ($j_\perp \ll 1$) and a model of free fermionic chains with interchain hopping. In both cases we find excellent agreement with our numerical results [30].

Results: In the following we present results of quantum quenches where the initial state of the system corresponds to the $j_\perp = 0$ ground state, whereupon at $t = 0$ we turn on a finite interchain coupling $j_\perp$. We focus mainly on results for infinitely long cylinders, leaving a discussion of the effect of finite chain number, N, until the end. We first address the question of what time scales we expect to feature in the quench. To provide a partial answer we turn to the quasiparticle causality picture of Refs. [1, 2, 33]. The energy imparted by the quench produces quasiparticle excitations which are entangled on a length scale $|\Delta|^{-1}$ along the chain. Intrachain scattering then only has an effect after a time, $t_\Delta = (2v\,|\Delta|)^{-1}$. On the other hand, the time scale governing interchain scattering can be estimated using Fermi's golden rule to be $t_{J_\perp} = |\Delta|^{1/2}\,(J_\perp R)^{-2}$. The final time scale of import is that encoding the chain length, R. This scale, given by $t_R \sim R/2v = |\Delta|\,Rt_\Delta$, describes the time for two quasiparticles, created at the same point and moving in opposite directions, to travel around a chain and then meet again. Hence there is a region, $t_\Delta, t_{J_\perp} < t < t_R$, where we may expect the time evolution to be representative of the 2D thermodynamic limit. But for $t > t_R$ the finite nature of the chains' circumferences will play a role. We stress that t_R does not govern the time scale for revivals in the system. Instead these occur on a much longer time scale, $t_{revival} \sim Nt_{J_\perp}$ where N is the number of chains in the system. Thus in our iTEBD simulations, we never expect to see strict revivals.

To illustrate these time scales in operation, we consider the occupation number, $n_i(x) = \psi_i^\dagger(x)\psi_i(x)$, for a fermionic mode on chain i, a simple measure of how the system departs from the initial state, for which $n_i(x) = 0$. In Fig. 2 we present how $n_i(x)$ evolves with time for a quench to $j_\perp = 0.1$. On the basis of our perturbative results for very small $j_\perp$ [30], we plot $n(x)$ in units of $j_\perp^2$ for all four quenches presented. These four quenches correspond to four different chain lengths, R.

We see that at short times, the results for $n_i(x)/j_\perp^2$ collapse onto a single curve as a function of t/t_Δ. As time increases, the curves cease to track one another. The first to do this is the $R = 4$ curve, then the $R = 6$ curve, and then finally the $R = 8$ curve. The time at which this happens corresponds, approximately, to t_R: the scale on which the quench explores the finite length of the chain. We expect small departures from this time scale because a finite $j_\perp$ will renormalize the quasiparticle velocity $v = 1$ in t_R. We also see from the inset of Fig. 2 that the evolution at longer times is no longer described by perturbation theory.

In Fig. 3 we explore a quench to a $j_\perp$ which exceeds j_c, the critical coupling for the $2+1$ dimensional system. Such a quench is among the most challenging numerically as the population of higher energy chain states becomes significant. Concomitantly, the time evolution is most dependent on E_c in this case. Ramped, rather than sudden, quenches can be implemented with some possible advantages in this regard [37], though we have not yet explored this possibility. Nonetheless in Fig. 3 we see that for a given chain length, R, we can find cutoffs, E_c such that the time evolution is converged.

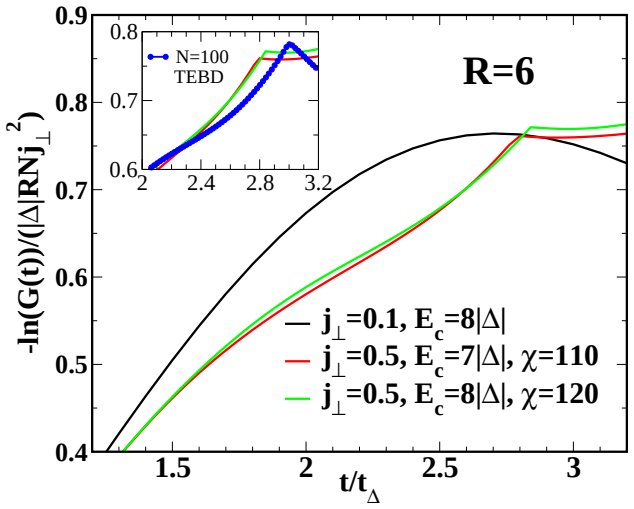

FIG. 4. Logarithm of return probability $G(t)$, for $R = 6$ for $j_\perp = 0.1, 0.5$. Non-analytic behaviour is seen at short times for a quench to $j_\perp = 0.5$. We find no non-analytic points for the corresponding quench to $j_\perp = 0.1$, even at longer times up to $t = t_\Delta = 10.0$ (not shown). Inset: comparison of the infinite chain number system data with a system with $N = 100$ chains computed using TEBD. The first non-analytic point for the infinite cylinder forms the edge of a plateau, whereas for a finite number of chains it takes the form of a peak.

It is also possible to calculate postquench correlations between the chains. We show the nearest neighbor spin–spin correlation function as a function of time, $\langle \sigma_i^z(x,t)\sigma_{i+1}^z(x,t)\rangle$, for a selection of R and $j_\perp$ in the inset of Fig. 3. Our choice of $j_\perp > 0$ favors antiferromagnetic correlations, producing the overall negative sign. An expansion in small t shows that this quantity is proportional to $j_\perp t^2$ allowing us to collapse the results onto a single curve at short times. Here we see signatures of both the $t_{J_\perp}$ and t_R scales. In the inset we have marked the intrachain scattering time $t_{J_\perp}$, for the system with $R = 8$ and $j_\perp = 0.1$. It is visible as the time that the $j_\perp = 0.1$ and $j_\perp = 0.01$ data begin to diverge. We also mark the time scale t_R at which the data for chains with $R = 8, j_\perp = 0.01$ begins to diverge from that of $R = 10, j_\perp = 0.01$.

To show that our method can handle non-trivial aspects of quenching through the critical coupling of the coupled chain system, we search for non-analyticities in the Loschmidt echo as a function in time. The 'Loschmidt echo' or overlap probability at a particular t is the modulus squared of the overlap between the initial and time evolved state:

$$G(t) = \left| \langle \Psi_0 | \, e^{-iH_{2\mathrm{DQI}}t} \, |\Psi_0\rangle \right|^2 \qquad (3)$$

where Ψ_0 is the ground state of the uncoupled chain system. In 1D it is useful to define a per site rate function, $\ell(t)$ via $G(t) = \exp[-N\ell(t)]$. Non-analyticities in $\ell(t)$ have been interpreted as 'dynamical phase transitions', following an exact calculation of this quantity for the 1D TFIM [38–40]. The general association of such non-analytic points with equilibrium critical phenomena is contested [41, 42], but we demonstrate analytically in low order perturbation theory[30] that for quenches to $j_\perp > 0.27$ we expect non-analyticities in $G(t)$. While this estimate for the value of $j_\perp$ is larger than j_c – because of the low order to which we took the computation – it does suggest that simple perturbation theory for the quantity $G(t)$ can be used to estimate the phase boundaries in some 2D quantum systems.

In Fig. 4 we plot $\log G(t)$ for a quench to $j_\perp = 0.5$ – a value of $j_\perp$ where we should see non-analyticities. In 2D this quantity scales with system volume RN, as does its 1D counterpart [38]. We also observe that it scales with $j_\perp^2$. As expected we find non-analytic behaviour for this quench, within the time window we are able to simulate, and see that the non-analyticity has the same qualitative structure for both $E_c = 7\,|\Delta|$ and $8\,|\Delta|$. For comparison we plot $\log G(t)$ for a quench to $j_\perp = 0.1$, where in contrast we find that this quantity is smooth within our simulation window. We remark that non-analyticities appear for the same quantity with $j_\perp = 0.2$ (not plotted), just above $j_c = 0.185$, but they first occur only at the edge of the attainable times with iTEBD.

Finally we consider the case of finite length and open boundary conditions. The TEBD algorithm is slower by approximately a factor of N due to the loss of translational invariance along the cylinder. We find negligible effect, for finite $N \gtrsim 10$ and i away from the ends of the cylinder, on the results for local quantities such as $n_i(x)$ (up to the time scales we reach). However this is not true for the Loschmidt echo (a global measure), especially when $|j_\perp| > j_c$. The inset of Fig. 4 shows the difference between the iTEBD and $N = 100$ results for $R = 6, j_\perp = 0.5$. While there is excellent agreement up to $t \sim t_\Delta$ (not shown), afterwards there is a clear change in the non-analytic point structure. We also find that this effect is even more pronounced for very small R and large N (where our model reduces to a single 1D TFIM), suggesting that boundary conditions have a non-negligible effect on the Loschmidt echo even for large systems. This last result has important consequences for possible experimental investigations.

Conclusions: We have demonstrated a robust method to compute dynamical behaviour in 2D quantum (d=2+1) systems after a quench, which we intend to use to study other systems including coupled quantum wires (i.e. coupled Luttinger liquids) and Heisenberg chains. The algorithm should prove especially useful when interpreting non-equilibrium cold atom [43, 44] and pump-probe experiments in the cuprates [45, 46].

We wish to acknowledge enlightening discussions with John Cardy, Fabian Essler, Andrew Goldsborough, Israel Klich, Anatoli Polkonikov, Rudolf Römer and Steve

Simons. This work was supported by the Engineering and Physical Sciences Research Council (grant number EP/L010623/1) and the US Department of Energy, Office of Basic Energy Sciences under Contract No. DE-AC02-98CH10886.

* andrew.james@ucl.ac.uk

[1] P. Calabrese and J. Cardy, Phys. Rev. Lett. **96**, 136801 (2006).

[2] P. Calabrese and J. Cardy, J. Stat. Mech. **2007**, P06008 (2007).

[3] M. Rigol, V. Dunjko, V. Yurovsky, and M. Olshanii, Phys. Rev. Lett. **98**, 050405 (2007).

[4] A. C. Cassidy, C. W. Clark, and M. Rigol, Phys. Rev. Lett. **106**, 140405 (2011).

[5] P. Calabrese, F. H. Essler, and M. Fagotti, Phys. Rev. Lett. **106**, 227203 (2011).

[6] P. Calabrese, F. H. Essler, and M. Fagotti, J. Stat. Mech. **2012**, P07016 (2012).

[7] P. Calabrese, F. H. Essler, and M. Fagotti, J. Stat. Mech. **2012**, P07022 (2012).

[8] F. H. Essler, S. Evangelisti, and M. Fagotti, Phys. Rev. Lett. **109**, 247206 (2012).

[9] J.-S. Caux and F. H. Essler, Phys. Rev. Lett. **110**, 257203 (2013).

[10] M. Fagotti, Phys. Rev. B **87**, 165106 (2013).

[11] S. Trotzky, Y.-A. Chen, A. Flesch, I. P. McCulloch, U. Schollwöck, J. Eisert, and I. Bloch, Nature Phys. **8**, 325 (2012).

[12] M. Greiner, O. Mandel, T. W. Hänsch, and I. Bloch, Nature **419**, 51 (2002).

[13] J. Eisert, M. Cramer, and M. B. Plenio, Rev. Mod. Phys. **82**, 277 (2010).

[14] U. Schollwöck, Ann. Phys. **326**, 96 (2011).

[15] E. Stoudenmire and S. R. White, Annu. Rev. Condens. Matter Phys. **3**, 111 (2012).

[16] M. P. Zaletel, R. S. Mong, C. Karrasch, J. E. Moore, and F. Pollmann, Phys. Rev. B. **91**, 165112 (2015).

[17] J. Haegeman, C. Lubich, I. Oseledets, B. Vandereycken and F. Verstraete, arXiv preprint arXiv:1408.5056 (2014).

[18] F. Verstraete and J. I. Cirac, arXiv preprint cond-mat/0407066 (2004).

[19] V. Murg, F. Verstraete, and J. I. Cirac, Phys. Rev. A **75**, 033605 (2007).

[20] H. N. Phien, I. P. McCulloch, and G. Vidal, arXiv preprint arXiv:1411.0391 (2014).

[21] R. M. Konik and Y. Adamov, Phys. Rev. Lett. **102**, 097203 (2009).

[22] A. J. A. James and R. M. Konik, Phys. Rev. B **87**, 241103 (2013).

[23] G. Vidal, Phys. Rev. Lett. **93**, 040502 (2004).

[24] F. H. L. Essler and R. M. Konik , From Fields to Strings: Circumnavigating Theoretical Physics, ed. M. Shifman, A. Vainshtein and J. Wheater, World Scientific, Singapore (2004).

[25] A. M. Tsvelik, Quantum Field Theory in Condensed Matter Physics Cambridge university press, (1995).

[26] V. P. Yurov and A. B. Zamolodchikov, Int. J. Mod. Phys. A **6**, 4557 (1991).

[27] R. M. Konik, Phys. Rev. Lett. **106**, 136805 (2011).

[28] M. Lässig, G. Mussardo and J. L. Cardy, Nucl. Phys. B **348**, 591 (1991).

[29] M. Lencsés and G. Takács, JHEP **052**, 1409 (2014).

[30] Supplemental Material, containing further details of the method and perturbative calculations, including a discussion of the appearance of non-analytic points in the Loschmidt echo.

[31] G. Vidal, Phys. Rev. Lett. **98**, 070201 (2007).

[32] R. Orus and G. Vidal, Phys. Rev. B **78**, 155117 (2008).

[33] P. Calabrese and J. Cardy, J. Stat. Mech. Theory. Exp. **2005**, P04010 (2005).

[34] S. Bravyi, M. B. Hastings and F. Verstraete, Phys. Rev. Lett. **97**, 050401 (2006).

[35] J. Eisert and T. J. Osborne, Phys. Rev. Lett. **97**, 150404 (2006).

[36] P. Fonseca and A. Zamolodchikov, J. Stat. Phys. **110**, 527 (2003).

[37] A sudden quench pumps more energy into the system relative to a ramped quench, and therefore will populate higher energy modes, reducing the efficiency of the algorithm.

[38] M. Heyl, A. Polkovnikov, and S. Kehrein, Phys. Rev. Lett. **110**, 135704 (2013).

[39] F. Pollmann, S. Mukerjee, A. G. Green, and J. E. Moore, Phys. Rev. E **81**, 020101 (2010).

[40] C. Karrasch and D. Schuricht, Phys. Rev. B **87**, 195104 (2013).

[41] M. Fagotti, arXiv preprint arXiv:1308.0277 (2013).

[42] F. Andraschko and J. Sirker, Phys. Rev. B **89**, 125120 (2014).

[43] K. Agarwal, E. G. D. Torre, B. Rauer, T. Langen, J. Schmiedmayer, and E. Demler, Phys. Rev. Lett. **113**, 190401 (2014).

[44] K. Agarwal, E. G. D. Torre, B. Rauer, T. Langen, J. Schmiedmayer, and E. Demler, Phys. Rev. Lett. **113**, 190401 (2014).

[45] S. Dal Conte, C. Giannetti, G. Coslovich, F. Cilento, D. Bossini, T. Abebaw, F. Banfi, G. Ferrini, H. Eisaki, M. Greven, A. Damascelli, D. van der Marel, and F. Parmigiani, Science **335**, 1600 (2012), http://www.sciencemag.org/content/335/6076/1600.full.pdf.

[46] J. D. Rameau, S. Freutel, L. Rettig, I. Avigo, M. Ligges, Y. Yoshida, H. Eisaki, J. Schneeloch, R. D. Zhong, Z. J. Xu, G. D. Gu, P. D. Johnson, and U. Bovensiepen, Phys. Rev. B **89**, 115115 (2014).